Observations and modelling of the UV and optical compact bursts in solar atmosphere

A. Berlicki[1,2]

[1]*Astronomical Institute, Czech Academy of Sciences, CZECH REPUBLIC,*
[2]*Astronomical Institute, University of Wrocław, POLAND arkadiusz.berlicki @asu.cas.cz*

Abstract
Compact brightenings or bursts (CBs) are commonly observed in the solar atmosphere, mainly in the new magnetic emerging flux areas. In the optical range they were reported hundred years ago as Ellerman bombs (EBs), and similar phenomena are also observed from space in the UV range. Analysis of the mutual relations between these structures observed in different spectral domains, from UV to microwaves, are crucial for better understanding small scale reconnection processes, which are believed to produce CBs. Multiwavelength observations, which take into account variety of the observed properties of CBs, can give us more precise information about their location and physical conditions. Especially, UV, optical and microwave (ALMA) radiation emitted from lower solar atmosphere provide unique diagnostic possibilities for studying magnetic reconnection and heating processes in lower solar atmosphere.

1. INTRODUCTION

Although short-lived compact bursts (CBs) are commonly observed in the solar atmosphere in many different spectral bands, their physics is still not completely understood. These bursts are believed to be caused by small-scale magnetic reconnections (Georgoulis et al. 2002, Pariat et al. 2004, 2009, Matsumoto et al. 2008, Zhao et al. 2017) that can heat plasma and drive its flows (Fig. 1).

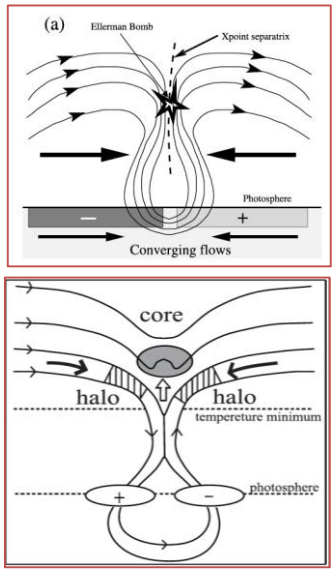

Figure 1. Possible magnetic field configurations leading to compact brightennings or Ellerman bombs appearance (Georgoulis et al. 2002, Matsumoto et al. 2008).

These phenomena appear mainly within solar active regions and display very intense, short-lived brightenings produced by plasma heated to temperatures of around 10^4 - 10^5 K (Peter et al. 2014). Therefore, they can be observed in the optical and ultraviolet (UV) spectral ranges (Fig. 2).

The temperature determined from observations suggests that CBs are located in the chromospheric parts of the solar atmosphere, with some extension towards the transition zone (TR) (Peter et al. 2014, Grubecka et al. 2016). In this context, the IRIS (Interface Region Imaging Spectrograph, De Pontieu et al. 2014) observations in far-UV (FUV) channel are important as they show many CBs-like events that are achieving transition region temperatures. A critical issue is then whether some UV CBs can reach coronal temperatures that would demonstrate that such events are not only testing grounds for magnetic reconnection theory, but may also be important for coronal heating. However, there are no detailed investigations of this phenomenon. In addition, due to the development of observing techniques in various spectral bands, the nomenclature of compact bursts is rather confused (see review paper of ISSI working group by Young et al. 2018).

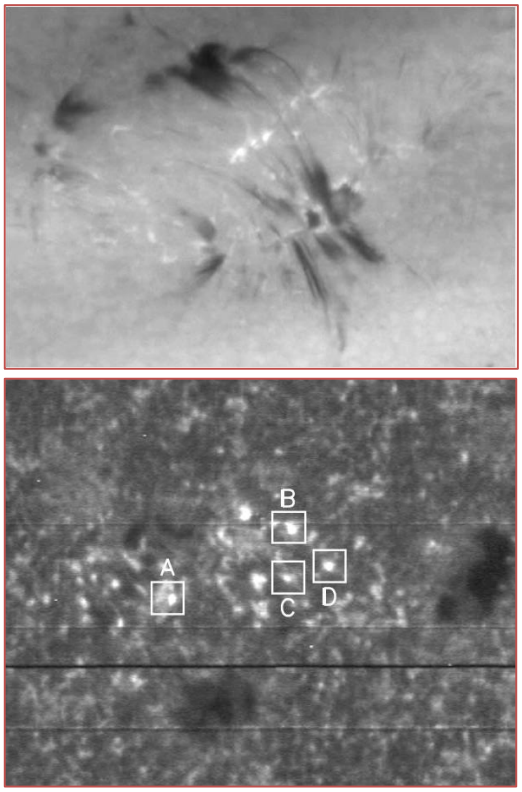

Figure 2. Example of compact brightenings observed in the optical range (EBs) and UV range.

2. PREVIOUS OBSERVATIONS AND MODELING

In the optical range these compact phenomena were observed historically by Ellerman (1917), and they are called as Ellerman bombs (EBs). They consist of short duration emissions that are spatially well localized and observed in the wings of chromospheric spectral line Hα. The Hα line profile of EBs is characterized by absorption at the line centre and strong emission in the wings with its maximum at Hα ± 1Å and fading at Hα ± 5Å (Fig. 3). This peculiar appearance of EBs is the reason for another name given to these patterns, "moustaches", as reported by Severny (1956).

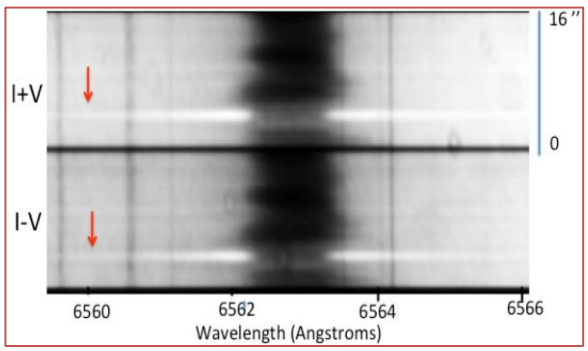

Figure 3. Example of typical Hα spectrum of Ellerman bomb (EBs).

EBs were frequently observed especially during the emergence of new active regions (Fig. 4). Different magnetic configurations have been proposed for EBs during flux emergence. Most of the EBs are associated with the inversion lines of small bipoles. Extrapolations suggest that the emerging loops have a sea-serpent shape with a succession of U and Ω loops (Pariat et al. 2004).

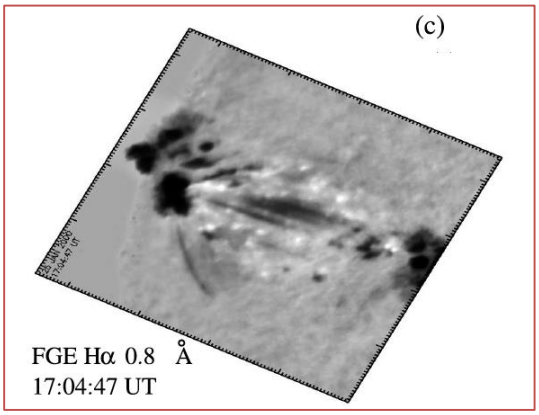

Figure 4. Example of EBs observed in the emerging active region (Georgulis et al. 2002).

Similar type of CBs are observed also in the UV spectral range (Grubecka et al. 2016, Tian et al. 2016). First, they were observed by the TRACE satellite in the UV continuum (Georgoulis et al. 2002), later by the UV telescopes on SDO/AIA space observatory, and more recently by the IRIS satellite (Tian et al. 2016). Observations of CBs obtained from IRIS led to faster progress in the analysis of their physical nature and mechanisms of radiation.

The line profiles and continua observed in EBs have been used in the past by a few authors to construct models of the atmosphere inside these structures. The results of this modelling imply that the whole region of EBs is hotter than a quiescent solar atmosphere, and the heating is significant only in the lower chromosphere or even photosphere (see review by Rutten et al. 2013), where the Hα line wings and UV continuum are formed. Fang et al. (2006) have obtained a semiempirical model of EBs, and they find that EBs require extra heating in the lower atmosphere, with about a 600-1300K temperature enhancement close to the temperature minimum region (Fig. 5). They also calculated that the total energy of EBs is about 10^{26} to 5×10^{27} erg, and they suggest that EBs could be similar to microflare events. However, they show a significant temperature increase even in regions of the middle and upper chromosphere, which should lead to a significant increase in the Hα line-center intensity, what is not observed in EBs.

Kitai (1983) performed NLTE (non-local thermo-dynamic equilibrium) calculations and derived theoretic-cal Hα line profiles emitted by different models of EBs. The models are characterized by a temperature and density increase located in the middle chromosphere. He was able to explain the basic characteristics of the spectra obtained at Hida Observatory.

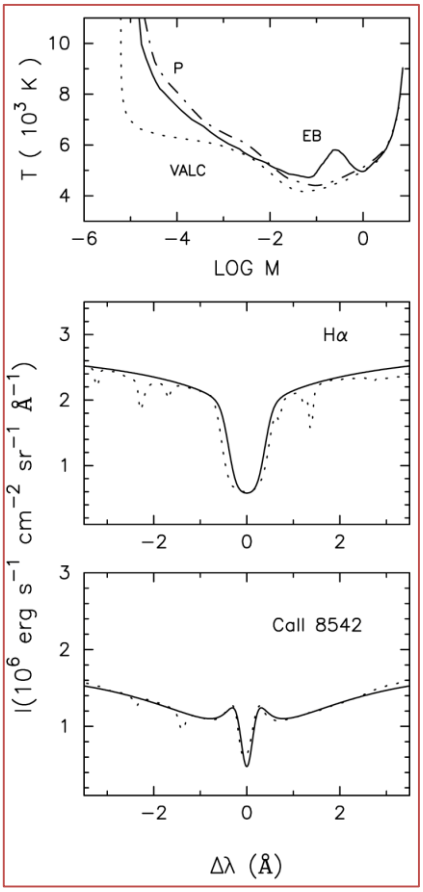

Figure 5. Temperature distributions in the semiempirical model (EB), compared to the plage model (P) and to the quiet-Sun model VAL-C by Vernazza et al. (1981). Below: The computed Hα and Ca II line profiles (solid lines) and the observed ones (dotted lines) (Fang et al. 2006).

Recently, Berlicki and Heinzel (2014) constructed a grid of 243 models of compact bursts based on 1D plane-parallel, semi-infinite atmosphere. These models were constructed by placing a local temperature increase (LTI, also known as a "hot-spot") structure at a given altitude in the solar atmospheric model of the quiet Sun. As a starting model they used the semi-empirical model C7 developed by Avrett & Loeser (2008). To find models which described the observed line spectra of CBs, they fit the observed Hα and CaII H line profiles with the theoretical profiles computed for all 243 models of the grid. With this method they found that the theoretical line profiles which fit the observations in the best way correspond to the model, where the "hot-spot" is located in lower chromosphere (Fig. 6).

3. NEW RESULTS FROM IRIS

The Interface Region Imaging Spectrograph (IRIS) with its high spatial resolution (pixel 0.167 arcsec, resolution of 0.3 arcsec), launched in June 2013 (De Pontieu

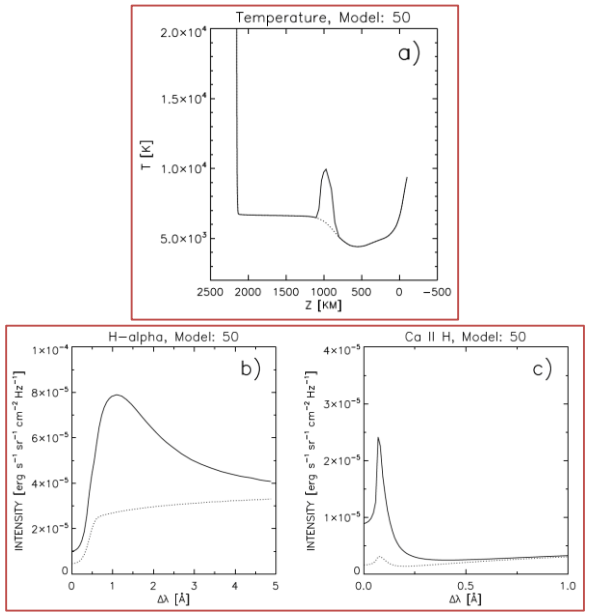

Figure 6. "Hot-spot" model of CBs and the corresponding theoretical Hα and Ca II H line profiles (Berlicki and Heinzel 2014).

et al. 2014) confirmed the existence of CBs in the Mg II h and k chromospheric lines, and also in Si IV, CII and the Mg II triplet lines, which are formed in a wide range of temperatures (Peter et al. 2014; Vissers et al. 2015). These bright features are very intriguing because they are not visible in O IV lines and the Si IV profiles are blended by photospheric lines that are visible in absorption. Peter et al. (2014) called them "hot explosions in the cool atmosphere". Fig. 7 presents the model of "hot explosions" proposed by Peter et al. (2014)

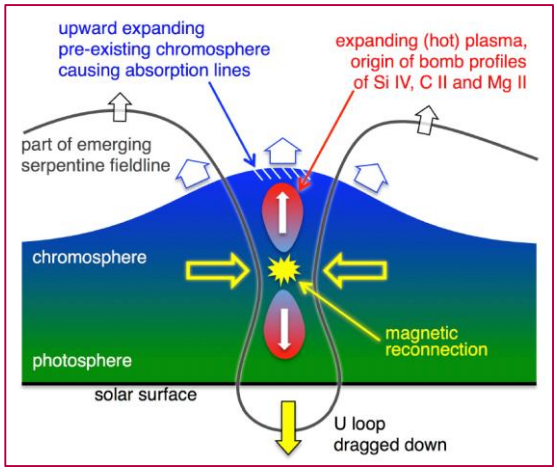

Figure 7. Model of "hot explosion" (or burst) proposed by Peter et al. (2014).

Vissers et al. (2015) investigated the IRIS signatures of Hα EBs. Among the large number of detected in Hα EBs in emerging regions, only a few of them were in the field of view of IRIS spectra and/or have an IRIS brightening counterpart signature.

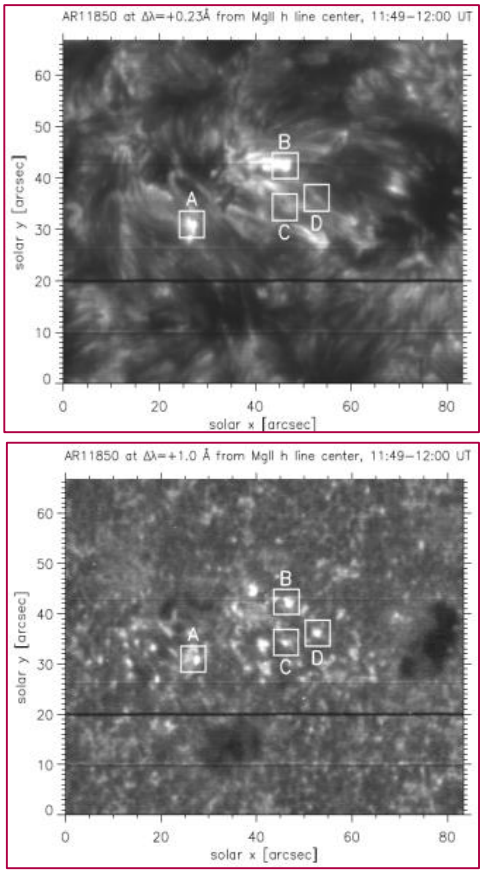

Figure 8. Reconstructed monochromatic images of the AR 11850 observed by IRIS obtained at 2803.7 Å (top panel) and 2804.5 Å (lower panel) (Grubecka et al. 2016).

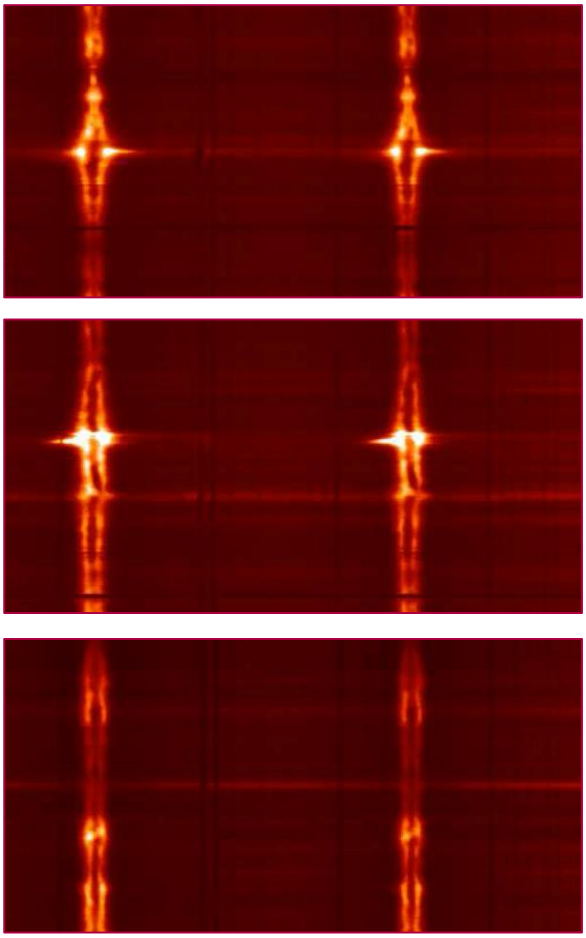

Figure 9. Examples of Mg II spectra from IRIS. (Grubecka et al. 2016)

In the paper of Grubecka et al. (2016) the authors had an opportunity to observe the emerging flux occurring in the AR NOAA 11850 located at N08, E10 on September 24, 2013 during the 60-day first joint observations of IRIS with the Télescope Héliographique pour l'Étude du Magnétisme et des Instabilités Solaires (THEMIS) magnetograph in Tenerife, and the Multi-channel Subtractive Double Pass (MSDP) spectrograph (Mein 1991) operating in the Meudon solar tower.

IRIS recorded two large dense rasters for 20 min, each covering the whole active region from 11:43 UT to 12:04 UT and from 15:39 to 15:59 UT on September 24, 2013. The pixel size is 0.167 arcsec. Both rasters (140 x 175 arcsec2) consist of 400 spectra with a step size of 0.35 arcsec and taken with a cadence of less than 3 s. The rasters are obtained in a large number of lines in the near ultraviolet NUV window: 2783 to 2834Å, and the two far ultraviolet windows: FUV1 1332-1348Å and FUV2 1390-1406Å wavelength bands. Fig. 8 presents examples of the reconstructed monochromatic images of the AR 11850 observed by IRIS. Several CBs can be seen in this active region.

From the observed AR, Grubecka et al. (2016) chose five CBs (A, B, C, D and E) for analysis. The processing of the UV IRIS spectra was performed in order to obtain calibrated Mg II, Si IV and C II line profiles for these CBs. In Fig. 9 examples of Mg II h and k line spectra of CBs are presented. Fig. 10 presents examples of the calibrated line profiles.

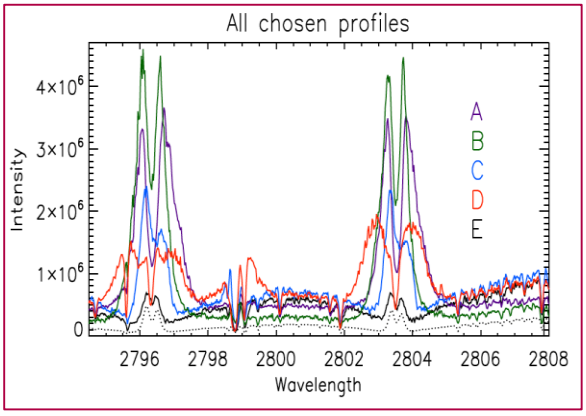

Figure 10. Plots of calibrated line profiles shown in a different colours: A purple; B green; C blue; D red; and E black. Intensity units is (erg/s/cm^2/Å/sr), wavelengths is in Å (Grubecka et al. 2016).

Next, Grubecka et al. (2016) used the grid of "hot-spot" models constructed by Berlicki and Heinzel (2014) and computed the synthetic Mg II h and k line profiles for all of them. After comparison and fitting with the calibrated Mg II line profiles, the corresponding models of CBs A, B, C, D and E were found. In Fig. 11 the example of fitting between theoretical and observed Mg II h line profiles is presented. The model corresponding to this fit is characterized by double-peak local temperature increase. This analysis suggests that CBs observed in the UV spectral range can be closely related with EBs observed in the visible light.

In summary, it is still not clear yet what is the structure of CBs in the context of ambient chromosphere and what are the relations between various types of radiation emitted from CBs. The time evolution of CBs and the relation between the structure of all compact phenomena observed in the optical range (EBs), UV range (IRIS bombs) and microwave range is still a subject of debate. Finally, the influence of the magnetic configuration and related reconnection on the appearance of different types of CBs is unknown. For more detailed discussion see Grubecka et al. (2016) and Young et al. (2018) papers.

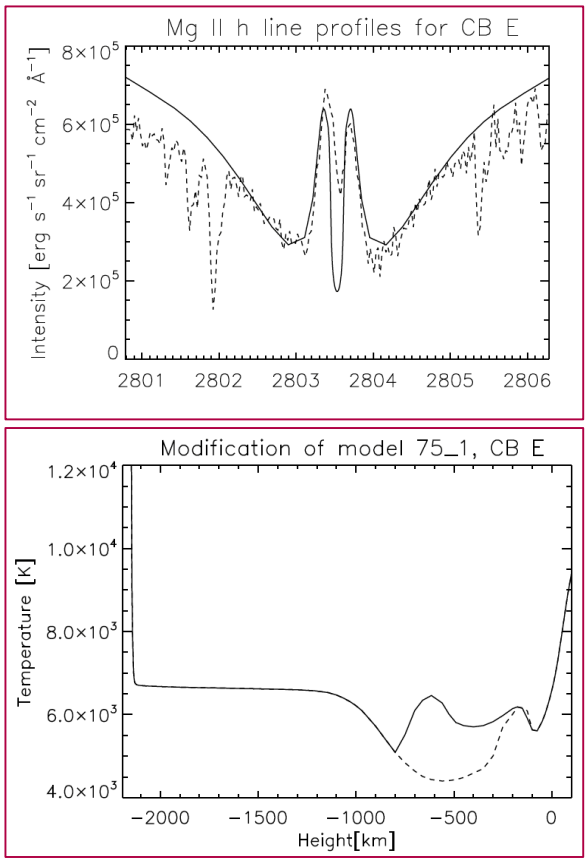

Figure 11. Upper panel: Example of the fitting of the theoretical (solid line) and observed (dashed line) Mg II h line profiles for CBs E. Lower panel: the model corresponding to this fit is presented (Grubecka et al. 2016)

4. ALMA VISIBILITY AND DIAGNOSTIC OF COMPACT BURSTS

One way to make progress in the CBs investigations is to use more spectral bands and to add those, which were not explored in the past, e.g. microwave range. Solar atmosphere can emit the microwave radiation as shown in NLTE simulations (Vernazza et al. 1981, Loukitcheva et al. 2006, Avrett and Loeser 2008). From this modelling it follows that the sub-millimeter/ millimetre (sub-mm/mm) waves arise from the middle or lower solar chromosphere. Until now, this millimetre spectral band was poorly investigated mainly due to the lack of high-resolution microwave instrumentation. A new possibility is now opened by ALMA instrument (http://www.almaobservatory.org/, Atacama Large Millimeter Array), which can observe the Sun in this range. The instrument can probe the solar chromosphere with the resolution well below 1 arcsec and therefore it should be possible to observe also these chromospheric compact bursts in the microwave spectrum.

CBs were never observed in sub-mm/mm radio wavelengths. There are also no papers where their potential visibility in this range is discussed. Due to the small spatial scales of CBs they could not have been observed with any existing radio instruments because no radio instrument at sub-mm/mm wavelength could achieve spatial resolution of the order of 1 arcsec. Therefore, ALMA gives us a great opportunity to obtain novel data which can be used to confirm CBs their thermal structure and location in the solar atmosphere.

One of the most interesting aspects of CBs physics is the relation between EBs observed in the optical range and CBs observed in ultraviolet. We expect that ALMA observations will provide us some additional information and gives us a great opportunity to obtain a novel data, which can be used to confirm CBs location and their thermal structure in the solar atmosphere.

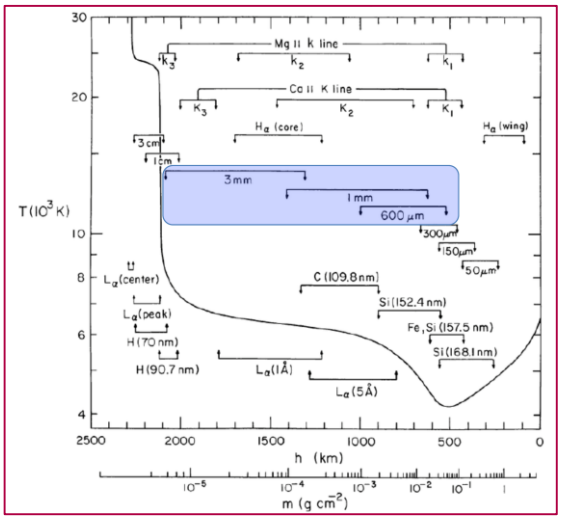

Figure 12. VAL-C model of the quiet-Sun atmosphere with the position of different lines and continua formation heights. (Vernazza et al. 1981). Blue contour marks mm/sub-mm continua.

Features of observed solar emission in microwave wavelengths give us several advantages. First of all, observations of the chromosphere in sub-mm/mm wavelengths are an important diagnostic of its physical conditions. The emission is almost entirely free-free, caused by free electrons colliding with ions and for optically thick features, this emission serves as an excellent thermometer – their brightness being simply proportional to the temperature of emitting gas (Wedemeyer et al. 2016).

The opacity is simple, well understood, and is in local thermodynamic equilibrium (LTE) with the electron density. In Fig. 12 heights of different continua and lines formation are represented (Vernazza et al. 1981). It is well seen that sub-mm/mm continuum emission if formed in middle and lower chromosphere and close to the temperature minimum. More precise calculations of the continuum formation height are represented in Fig. 13 (Avrett and Loeser 2008).

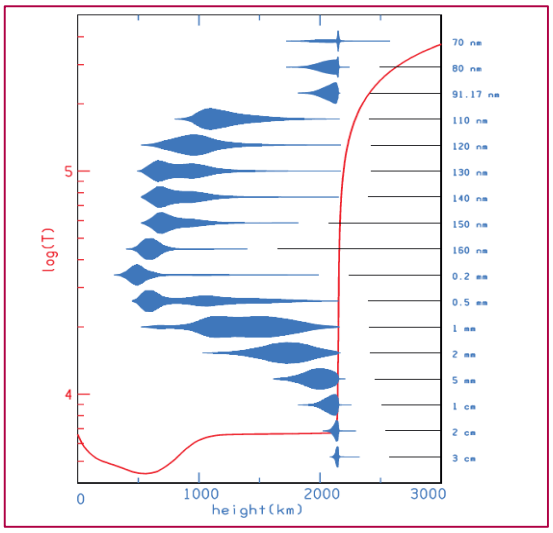

Figure 13. Heights of different continua formation computed for semiempirical C7 model of the solar atmosphere (Avrett and Loeser 2008).

Since there are no previous radio observations of CBs, in order to be sure that CB structures will be observed by ALMA at 1- and 3-mm wavelengths (band 6 and 3), we performed preliminary simulations using the NLTE radiative transfer codes. We used three different "hot-spot" models of CBs adapted from Berlicki and Heinzel (2014). Model 1: CB in the chromosphere, Model 2: CB around the temperature minimum region, Model 3: CB close to the photosphere - Fig. 14 (upper panel). Then, using NLTE radiative transfer codes we determined their brightness temperature (T_B) in wavelengths corresponding to already used ALMA band 3 (3 mm) and 6 (1 mm), and for two other channels (6 mm and 0.45 mm), which can be used in future solar observations (Tab. 1).

We compared the obtained T_B for all CBs with brightness temperature calculated for C7 model (Avrett & Loeser 2008) of the quiet-Sun atmosphere. In Fig. 14 (lower panel) we present the theoretical brightness temperature contrast C of CBs structures with respect to the quiet-Sun (QS) as a function of wavelength calculated for these three models of CBs.

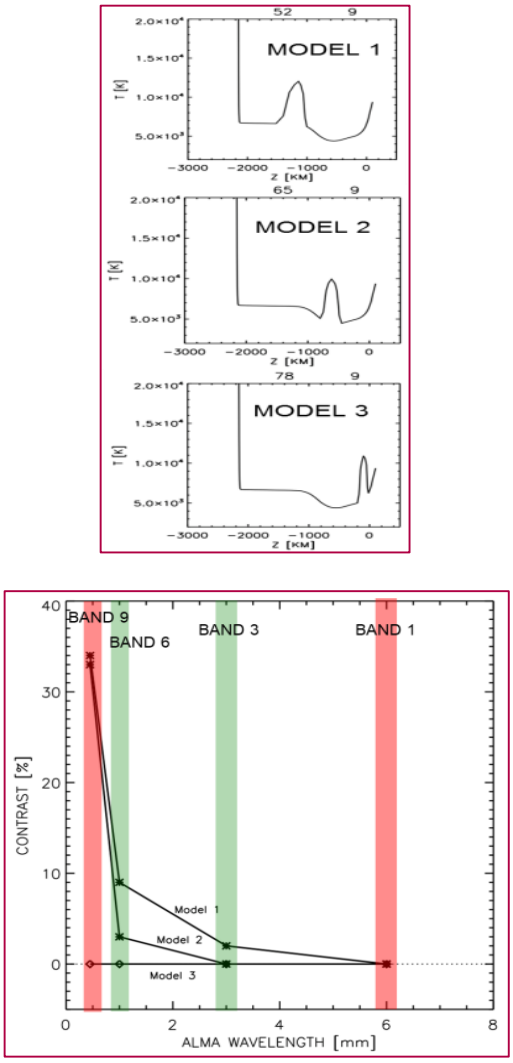

Figure 14. Representative "hot-spot" models used for NLTE calculation of CBs visibility in sub-mm/mm waves (upper panels) and the simulated contrast for three models of CBs for different ALMA bands (below). Green colors mark the ALMA band 3 and 6 already used for solar observations.

The contrast C is defined as:

$$C = (T_{CB} - T_{QS}) / T_{QS}, \qquad (1)$$

where T_{CB} is the brightness temperature of CB observed at a given moment of time, and T_{QS} is the brightness temperature of the quiet-Sun atmosphere.

From the plots in Fig. 14 and from Tab. 1 we can conclude that we will not see CBs if they are located in the photosphere (Model 3) because of very low contrast with respect to the quiet Sun. CBs located higher and

higher should be progressively observed in shorter ALMA wavelengths, and CBs located in the chromosphere should be visible in almost all ALMA bands (except the 6 mm channel). Considering our previous results that CBs are located in the lower chromosphere we can see that some CBs will be visible by ALMA in band 3 and 6 and the visibility of CBs in different ALMA channels can give us important constrains on their formation altitude in the solar atmosphere.

Model	λ=0.45 mm (band 9)	λ=1 mm (band 6)	λ=3 mm (band 3)	λ=6 mm (band 1)
C7 (QS)	T_B=5370 K $h_{(\tau=1)}$=950 km	T_B=6330 K $h_{(\tau=1)}$=1100 km	T_B=6760 K $h_{(\tau=1)}$=1400 km	T_B=6810 K $h_{(\tau=1)}$=1520 km
1 Hot-spot 52_9 (high chr.)	T_B=7210 K $h_{(\tau=1)}$=1400 km	T_B=6930 K $h_{(\tau=1)}$=1620 km	T_B=6880 K $h_{(\tau=1)}$=1820 km	T_B=6790 K $h_{(\tau=1)}$=1890 km
2 Hot-spot 65_9 (middle chr.)	T_B=7130 K $h_{(\tau=1)}$=700 km	T_B=6500 K $h_{(\tau=1)}$=1140 km	T_B=6780 K $h_{(\tau=1)}$=1400 km	T_B=6810 K $h_{(\tau=1)}$=1520 km
3 Hot-spot 78_9 (low chr.)	T_B=5380 K $h_{(\tau=1)}$=350 km	T_B=6350 K $h_{(\tau=1)}$=1100 km	T_B=6770 K $h_{(\tau=1)}$=1400 km	T_B=6810 K $h_{(\tau=1)}$=1520 km

Table 1. Brightness temperature and τ=1 depth for given wavelength obtained from NLTE modelling. Numbers 1, 2, 3 in first column correspond to Model 1, 2 and 3.

5. SUMMARY

Even if CBs are small solar structures, their role in the atmospheric heating can be significant (Peter et al. 2014). They are observed in regions of the magnetic flux emergence (Archontis and Hood 2009), or at the ends of chromospheric fibrils forming superpenumbra around large sunspots. They occur not only in a new active region but also in those where the magnetic field starts to rebuild. Georgoulis et al. (2002) found that CBs tend to concentrate above the magnetic neutral lines outlining the boundaries of supergranular cells or in MDF (moving dipolar features, Bernasconi et al. 2002). Almost all of these events are believed to be driven by subsurface flow patterns that drive the above-surface magnetic field into a configuration whereby the magnetic reconnection can take place. This magnetic reconnection occurs at smaller spatial and energetic scales than in magnetic reconnections producing solar flares. Also, the magnetic configuration leading to the reconnection can be different (Watanabe et al. 2008). Therefore, analysis of less energetic CBs can give us some additional information on these processes, which can be compared with the flare conditions.

Numerical simulations also show that compact brightenings (CBs) can be visible in different ALMA frequency bands. The computed brightness temperature T_B of CBs depends on the assumed model of the "hot-spot" and it is larger than the quiet-Sun value. The higher distance of the "hot-spot" from the photosphere, the larger contrast of in all bands. Therefore, observations of CBs with ALMA interferometer can significantly help us in understanding of their physics. However, one has to remember that ALMA observations can be even more valuable when obtained together with other observations of the chromosphere obtained e.g. with IRIS (in Mg II and hotter Si IV and C II lines), SDO (magnetograms, continuum images), and ground-based solar observatories in Hα, Ca II H and K lines, He I 1083 nm, magnetic field maps, G-band, etc). All these co-temporal and multiwavelength observations can be complemented by the theoretical modelling of CBs using static or time-dependent numerical NLTE codes. Only interpretation of observations with theoretical calculations can provide a complete picture of CBs phenomena.

Acknowledgements

This work was supported by the grant No. 16-18495S of the Grant Agency of the Czech Republic, by the project LM2015067 and by the institutional grant RVO 67985815.

REFERENCES

Archontis, V. and Hood, A. W.: 2009, A&A, 508, 1469
Avrett, E. H., Loeser, R.: 2008, ApJS, 175, 229
Berlicki, A., Heinzel, P.: 2014, A&A, 567, 110
Bernasconi, P. N., Rust, D. M., Georgoulis, M. K., Labonte, B. J.: 2002, Solar Phys., 209, 119
De Pontieu, B., Title, A.M., Lemen, J. R., et al.: 2014, Solar Phys., 289, 2733
Ellerman, F.: 1917, ApJ, 46, 298
Fang, C., Tang, Y. H., Xu, Z., Ding, M. D., & Chen, P. F.: 2006, ApJ, 643, 1325
Georgoulis, M. K., Rust, D. M., Bernasconi, P. N., Schmieder, B.: 2002, ApJ, 575, 506
Grubecka, M., Schmieder, B., Berlicki, A., Heinzel, P., Dalmasse, K., Mein, P.: 2016, A&A, 593, 32
Kitai, R.: 1983, Sol. Phys., 87, 135
Loukitcheva, M. Solanki, S. K., and White, S.: 2006, A&A, 456, 713
Matsumoto, T., Kitai, R., Shibata, K., et al.: 2008, PASJ, 60, 95
Mein, P. 1991, A&A 248, 669
Pariat, E., Aulanier, G., Schmieder, B., et al.: 2004, ApJ, 614, 1099
Pariat, E., Masson, S., Aulanier, G.: 2009, ApJ, 701, 1911
Peter, H., Tian, H., Curdt,W., et al.: 2014, Science, 346, 1255726
Rutten, R.J., Vissers, G.J.M., Rouppe van der Voort, L.H.M., Sütterlin, P., & Vitas, N.: 2013, Journal of Physics Conference Series, 440, 012007
Severny, A. B.: 1956, The Observatory, 76, 241
Tian, H., Xu, Z., He, J., & Madsen, C.: 2016, ApJ, 824, 96
Watanabe, H., Kitai, R., Okamoto, K., Nishida, K., Kiyohara, J., Ueno, S., Hagino, M., Ishii, T. T., Shibata, K.: 2008, ApJ, 684, 736
Wedemeyer, S.: 2016, Space Sci. Rev. 200, 1
Vernazza, J. E., Avrett, E. H., and Loeser, R.: 1981, Astrophysical Journal Supplement Series, 45, 635
Vissers, G. J. M., Rouppe van der Voort, L. H. M., Rutten, R. J., Carlsson, M., De Pontieu, B.: 2015, ApJ, 812, 11
Young, P. R., Tian, H., Peter, H., Rutten, R. J., Nelson, C. J., Huang, Z., Schmieder, B., Vissers, G. J. M., Toriumi, S., Rouppe van der Voort, L. H. M., Madjarska, M. S., Danilovic, S., Berlicki, A., Chitta, L. P., Cheung, M. C. M., Madsen, C., Reardon, K. P., Katsukawa, Y., Heinzel, P.: 2018, Review article accepted for publication in Space Science Reviews (eprint arXiv:1805.05850, https://arxiv.org/abs/1805.05850)
Zhao, J., Schmieder, B., Li, H., Pariat, E., Zhu, X., Feng, L., Grubecka, M.: 2017, ApJ, 836, 52